Geophysical Journal International

Geophys. J. Int. (2012) **190,** 1271–1278 doi: 10.1111/j.1365-246X.2012.05559.x

Relative arrival-time upper-mantle tomography and the elusive background mean

Ian D. Bastow

School of Earth Sciences, University of Bristol, Bristol, BS8 1RJ, UK. E-mail: ian.bastow@bristol.ac.uk

Accepted 2012 May 28. Received 2012 May 28; in original form 2011 June 23

SUMMARY

The interpretation of seismic tomographic images of upper-mantle seismic wave speed structure is often a matter of considerable debate because the observations can usually be explained by a range of hypotheses, including variable temperature, composition, anisotropy, and the presence of partial melt. An additional problem, often overlooked in tomographic studies using relative as opposed to absolute arrival-times, is the issue of the resulting velocity model's zero mean. In shield areas, for example, relative arrival-time analysis strips off a background mean velocity structure that is markedly fast compared to the global average. Conversely, in active areas, the background mean is often markedly slow compared to the global average. Appreciation of this issue is vital when interpreting seismic tomographic images: 'high' and 'low' velocity anomalies should not necessarily be interpreted, respectively, as 'fast' and 'slow' compared to 'normal mantle'. This issue has been discussed in the seismological literature in detail over the years, yet subsequent tomography studies have still fallen into the trap of mis-interpreting their velocity models. I highlight here some recent examples of this and provide a simple strategy to address the problem using constraints from a recent global tomographic model, and insights from catalogues of absolute traveltime anomalies. Consultation of such absolute measures of seismic wave speed should be routine during regional tomographic studies, if only for the benefit of the broader Earth Science community, who readily follow the red = hot and slow, blue = cold and fast rule of thumb when interpreting the images for themselves.

Key words: Tomography; Body waves; Seismic tomography; Cratons; Hotspots.

1 INTRODUCTION

1.1 Overview

Constraining accurately the amplitudes of seismic wave speed anomalies is particularly desirable to seismologists since this information can subsequently be used to develop hypotheses concerning the physical state of the mantle (e.g. temperature, partial melt, composition and anisotropy: Karato 1993; Sobolev *et al.* 1996; Goes *et al.* 2000; Takei 2002; Artemieva *et al.* 2004; Anderson 2011). Seismic tomography is a commonly used method to achieve this, but tomographic images can be generated in a variety of ways, with each yielding fundamentally different information about subsurface seismic wave speed structure. Surface-wave methods, for example, can be used to constrain absolute seismic wave speed anomalies across a region with good depth resolution (e.g. Tanimoto & Anderson 1985; Zhang & Lay 1996; Ritzwoller *et al.* 2002; Pilidou *et al.* 2005; Priestley *et al.* 2008). However, they lack the high-quality lateral resolution afforded by higher-frequency body-wave studies, which are thus an extremely commonly used tool for the study of regional upper-mantle seismic wave speed structure (e.g. VanDecar 1991; Tilmann *et al.* 2001; Allen *et al.* 2002; Bastow *et al.* 2005; Rawlinson & Kennett 2008).

In the case of temporary seismograph networks, high levels of background noise, and the emergent (as opposed to impulsive) nature of many body-wave phase arrivals (Fig. 1), means it is often impossible to identify accurately the onset of *P*-wave or *S*-wave energy, and thus the absolute traveltime anomaly (t_{abs}) for a given station-earthquake pair. Many studies thus instead compute relative arrival-times (e.g. VanDecar 1991; Tilmann *et al.* 2001; Allen *et al.* 2002; Bastow *et al.* 2005; Rawlinson & Kennett 2008). These are times that have been normalized by the removal of a mean arrival-time for a given earthquake from each station of a regional network (e.g. Romanowicz 1979; Aki & Richards 1980).

In the relative arrival-time approach, seismic phases are picked on seismograms at the first identifiable peak or trough in the first cycle of coherent energy across a network (Fig. 1). The similarity of teleseismic waveforms then lends itself naturally to the use of multichannel cross-correlation techniques (e.g. VanDecar & Crosson 1990) to compute relative arrival-times to an extremely high degree of accuracy (Fig. 2). Thus, while absolute traveltime anomalies (t_{abs}), computed from the first arriving phase energy (t_{fb}) are

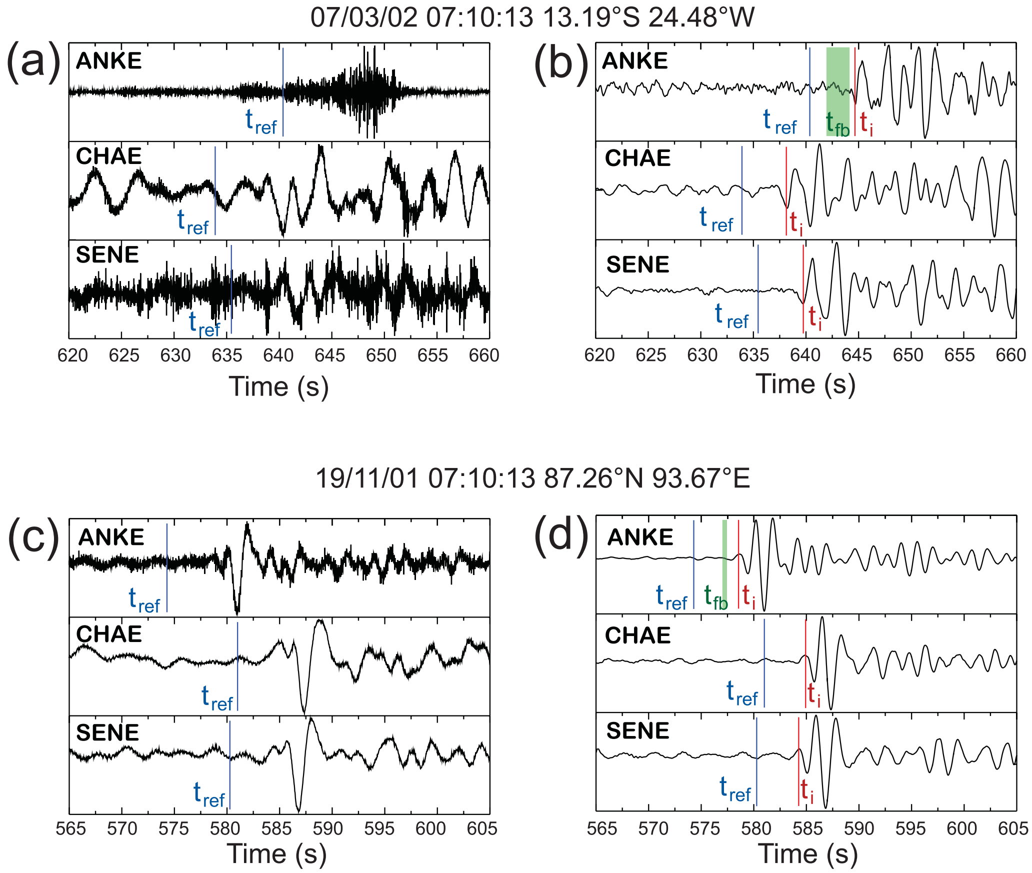

Figure 1. Examples of vertical component P-wave seismograms; 40 s of data are shown. Panel (a) shows a noisy P waveform recorded at three temporary seismograph stations in Ethiopia deployed during the Ethiopia Afar Geoscientific Lithospheric Experiment (EAGLE, see e.g. Bastow *et al.* 2011). Panel (b) shows the same waveforms after application of a zero-phase two-pole Butterworth bandpass filter with corner frequencies of 0.4 and 2 Hz. Panel (c) is an unfiltered example of the best quality data recorded at EAGLE stations. The waveforms in panel (d) are the filtered traces. The P wave picks labelled on each figure are the expected traveltimes according to the IASP91 traveltime tables. The later arriving red picks are those that would typically be used during relative arrival-time analysis (see e.g. VanDecar & Crosson 1990). The first break of energy, shown by the green bars (the absolute traveltime, t_{fb}) is particularly difficult to identify in panels (a–c). More impulsive, high signal-to-noise ratio waveforms, such as panel (d), are relatively uncommon in short-duration temporary deployments; hence the popularity of the relative arrival-time approach.

defined as

$$t_{\mathrm{abs}} = t_{fb} - t_{ref}, \tag{1}$$

the relative phase arrival-time (t_{rel}) for station i, for a given earthquake is given by

$$t_{\mathrm{rel}} = t_i - \bar{t}, \tag{2}$$

where t_i is the phase pick time for station i (Figs 1 and 2), and $\bar{t}$ is the mean phase pick time for all stations across the seismograph network for a given earthquake. The tomographic images that result from the inversion of such data provide detailed information about the morphology of mantle seismic wave speed anomalies; their amplitudes though, are significantly more difficult to interpret. Even after the (generally amplitude reducing) effects of inversion regularization are considered, it must be born in mind that the background mean velocity structure for a region is lost entirely during the computation of t_{rel}, with the implication that low and high velocity structure in these models (often shown as red and blue, respectively) can usually not be interpreted as genuinely slow or fast compared to the global mean. This problem has been well documented before (e.g. Aki *et al.* 1977; Evans & Achauer 1993; Lévêque & Masson 1999; Foulger 2010), yet unfamiliarity with the issue has since still resulted in markedly different interpretations in co-located regional tomographic studies. In addition to highlighting examples of this, I provide here a simple strategy to help address the zero-mean problem using constraints from a recent global tomographic model, and insights from catalogues of absolute traveltime anomalies.

1.2 Relative arrival-time tomography and implications for $\delta V = 0$ per cent

The first 3-D inversion method for retrieving velocity structure from the traveltimes of seismic body waves recorded by a seismic array (the NORSAR array in southern Norway) was developed in the 1970's by Aki, Christofferson and Husebye (Aki *et al.* 1976, 1977) and is known simply as the 'ACH' method. ACH uses relative-arrival times for two principal reasons. First, relative arrival-times do not require identification of the first breaking energy on a seismogram—instead, the first clear peak or trough of energy can be picked and cross correlation techniques used to align the traces accurately for a given earthquake recorded across a network (Fig. 2). Secondly, relative arrival-times isolate the lateral variations in traveltimes due

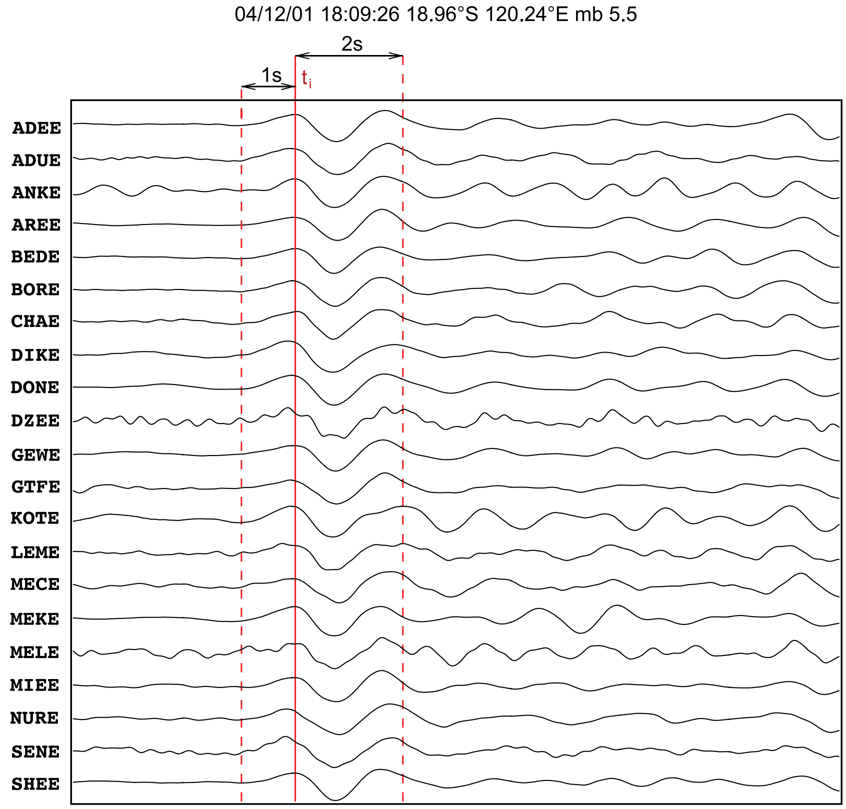

Figure 2. Bandpass filtered seismic traces. Traces have been aligned with respect to a cross-correlation optimized pick (solid red line) of the initial packet of P-wave energy. All traces have been bandpass filtered with a zero phase Butterworth filter with corner frequencies of 0.4–2 Hz. The vertical dashed lines indicate the 3 s window of data used in the cross-correlation procedure.

to mantle structures directly beneath a seismograph network (the depth range of this region is governed by the aperture of the network and can be up to several hundreds of kilometres; e.g. Evans & Achauer 1993). Because the rays for a given earthquake sample essentially the same Earth structure at large distances from the regional network, uncertainties in hypocentre information (source mis-locations and origin time errors) and the effects of un-resolvable source-side Earth structure are removed from the traveltime data set. This reduces the opportunity for un-warranted structure to be mapped into the region of interest.

In the years since ACH, body-wave traveltime inversion ray-theory techniques have been developed that adopt more sophisticated parametrization schemes (smoothed splines as opposed to blocks), ray geometries (curved as opposed to straight ray-paths) and regularization schemes (smoothing and flattening as well as amplitude damping; e.g. VanDecar *et al.* 1995; Allen *et al.* 2002; Rawlinson & Kennett 2008). As with the ACH method, the relative arrival-time data are inverted for a velocity structure assuming some starting 1-D velocity model (based, for example, on the IASP91 traveltime tables of Kennett & Engdahl 1991) to compute initial ray-paths through the Earth.

The use of relative arrival-time data has important consequences for the resulting tomographic images. First, the zero mean of the resulting velocity model will rarely be the same as the global mean (e.g. Aki *et al.* 1977; Lévêque & Masson 1999). Some studies use additional seismological constraints such as surface-wave data to help constrain the background starting model (e.g. Allen *et al.* 2002; Rawlinson & Fishwick 2011), but usually this information is not incorporated formally into the inversion and 'standard' Earth 1–D models are thus assumed instead. Relatively low and high wave speed areas in the final tomographic model (often shown as red and blue, respectively) cannot always, therefore, be interpreted as genuinely 'fast' and 'slow', respectively, compared to 'normal' mantle. A second problem with ACH-type inversions is that they can only estimate velocity contrasts in the horizontal direction; vertical velocity variations cannot, in a strict mathematical sense, be resolved (e.g. Lévêque & Masson 1999). If an anomalously fast or slow wave speed layer characterizes a given depth range beneath a regional network, its influence on the final inversion will be entirely removed during the computation of the relative arrival-times from the subvertical rays. This is illustrated in Fig. 3, where a network-wide low velocity zone at 200 km is demonstrated to be irretrievable using relative-arrival time tomography. A large, flat, fast wave speed slab would also be invisible during relative arrival-time analysis.

Fig. 4 highlights the difficulties in comparing tomographic images from different tomographic studies. In Fig. 4(b) a slice at 150 km depth through the global tomographic model of Ritsema *et al.* (2010) can readily be used to identify seismically fast shields in blue, which contrast with the seismically slow hotspots. Fig. 4(a) shows a slice at the same depth through the regional P-wave relative arrival-time tomographic model of Frederiksen *et al.* (2007) in the Canadian shield. The same study area is characterized in the global model by markedly fast wave speed anomalies (Fig. 4b) so red areas in Fig. 4(a) are, in reality, probably fast compared to the global mean. This assertion is corroborated by the study of van der Lee & Fredericksen (2005), whose NA04 velocity model for the North American continent indicates fast velocity structure for the entire region resolved in Fig. 4(a) (except, perhaps, for the region south of ∼45°N where a southward transition to normal and then

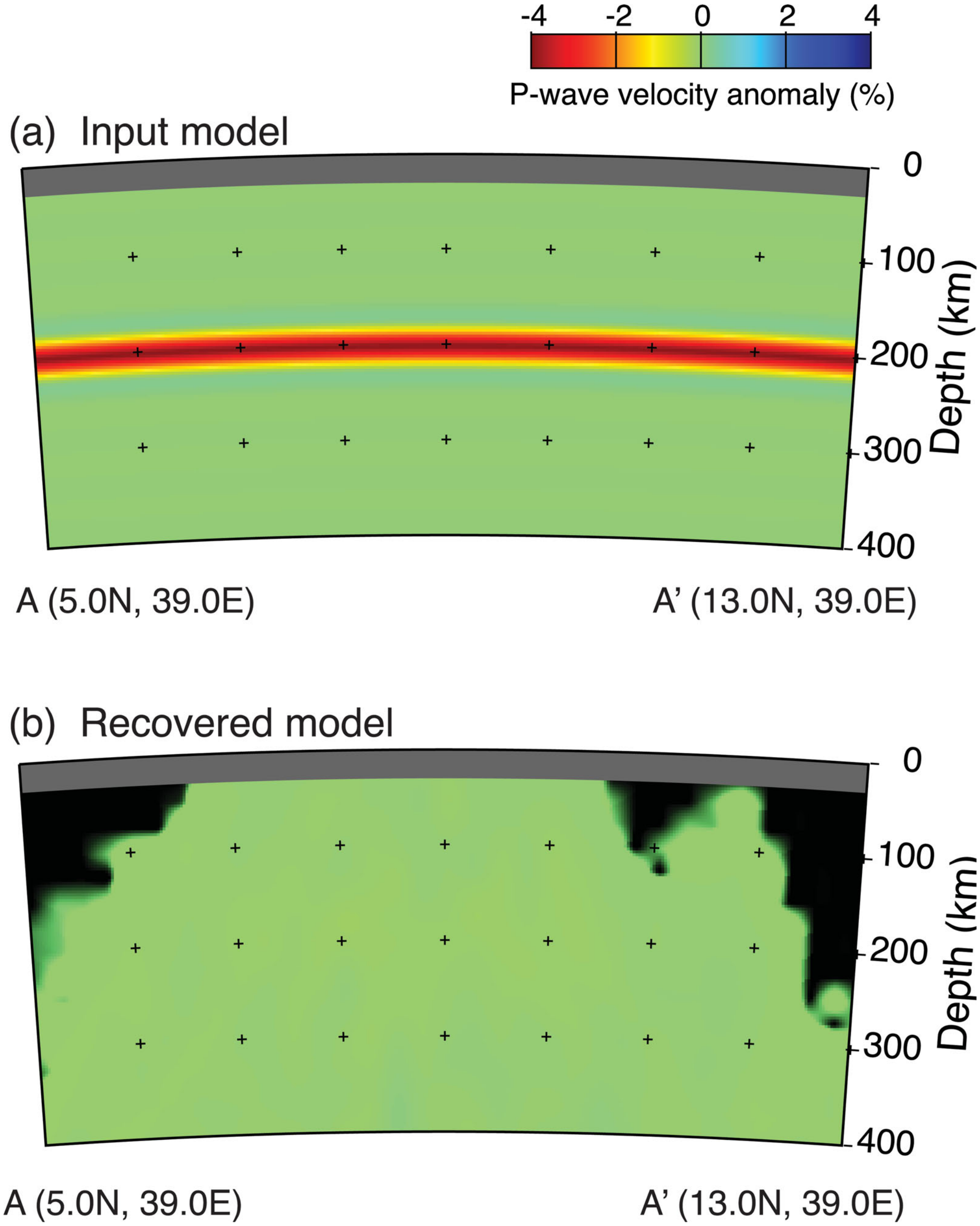

Figure 3. A synthetic velocity model consisting simply of a $\delta V_P = –4$ per cent low velocity zone at 200-km-depth beneath Ethiopia. Tomographic inversion (using the method of VanDecar *et al.* 1995) of relative arrival-time residuals through this model results in a final velocity model with no structure. The influence of the layer is lost entirely during the computation of the traveltime data set. Even if absolute traveltimes were used instead, the subvertical rays would still be completely unable to resolve the layer. Station–earthquake pairs used in the inversion are the same as in the study of Bastow *et al.* (2008). A Gaussian residual time error component with a standard deviation of 0.02 s was added to the theoretical *P*-wave traveltimes to simulate the uncertainties often encountered in observed data. Areas of poor ray coverage are black.

slower structure occurs). Frederiksen *et al.* (2007) are thus entirely correct to refer in their manuscript to red regions as ‘low’, not ‘slow’ velocity anomalies. The same correct terminology is used by Sol *et al.* (2002) in their tomographic study of Western Superior upper-mantle seismic structure—a study area even closer to the heart of the Canadian shield.

Figs 4(b) and (c) highlight a similarly extreme example of the zero mean problem in Ethiopia, East Africa. While the global model identifies Ethiopia as a region of markedly low seismic wave speed, the depth slice through the regional model of Bastow *et al.* (2008) highlights both high and low wave speed anomalies, precisely as is expected in a relative arrival-time tomographic model. Bastow *et al.* (2005, 2008) noted that International Seismological Catalogue (ISC) traveltime data for permanent station AAE (Addis Ababa) in Ethiopia show that mean *P*-wave traveltime delays there (4.6 ± 0.15 s with respect to the IASP91 traveltime tables) are amongst the latest worldwide, with the implication that the mantle beneath the region may be amongst the slowest on Earth (an observation also made in the 1980s by surface wave studies such as Nakanishi & Anderson (1984)). The zero mean for Figs 4(b)

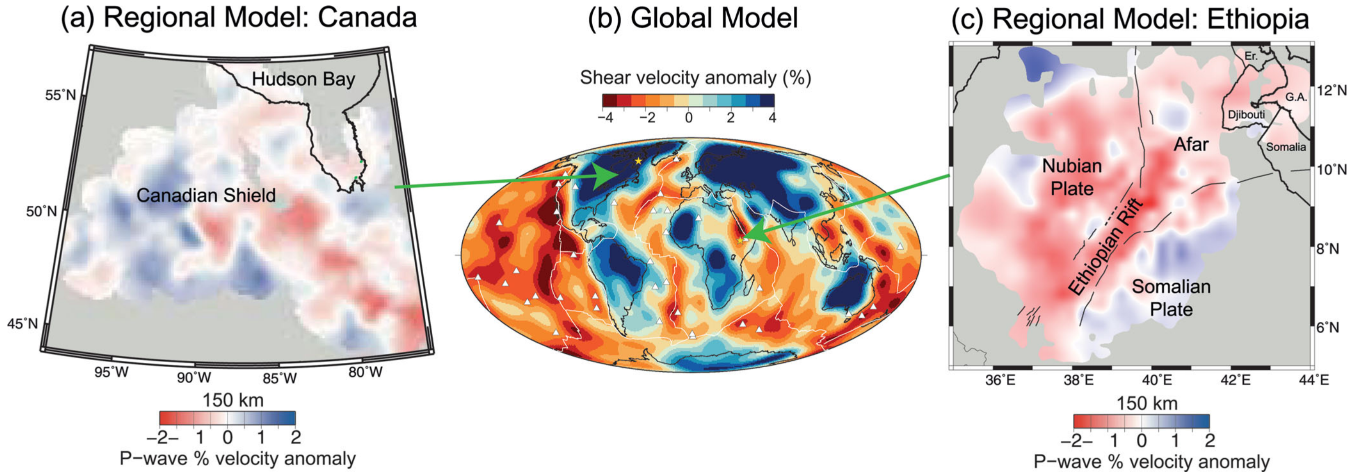

Figure 4. A comparison of global and regional tomographic models. Panel (A) Slice at 150-km-depth through the *P*-wave relative arrival-time tomographic model of Frederiksen *et al.* (2007) in Canada, computed from the inversion of relative arrival-time residuals. Panel (B) Slice at 150-km-depth through the global tomographic model of Ritsema *et al.* (2010). White lines are plate boundaries. Panel (C) Slice at 150-km-depth through the *P*-wave relative arrival-time tomographic model of Bastow *et al.* (2008) in Ethiopia, computed from the inversion of relative arrival-time residuals. Dark lines are mid-Miocene border faults that define the Ethiopian Rift. Areas of poor ray coverage are black.

and (c) are thus probably as different as is possible anywhere on Earth. Even high wave speed anomalies presented by Bastow *et al.* (2008) are likely to be markedly slow compared to normal mantle.

2 RECENT MANIFESTATIONS OF THE ZERO MEAN PROBLEM

In a recent study using broadband seismic and data from Ireland, O'Donnell *et al.* (2011) suggest that compositional contrasts and small-scale convection likely dominate their upper-mantle relative arrival-time seismic tomographic images, with no requirement for elevated temperatures beneath the region. This was in contrast to earlier interpretations of regional tomographic images by Wawerzinek *et al.* (2008) and Arrowsmith *et al.* (2005) who cited low wave speed anomalies as evidence for hot (up to ∼200 °C), partially molten Iceland plume material ponding beneath lithospheric thin spots. These interpretations are markedly different, and the discordance stems entirely from the studies' different assumptions about the region's zero mean velocity structure. While Arrowsmith *et al.* (2005) and Wawerzinek *et al.* (2008) interpreted low wave speed anomalies as slow compared to the global average, O'Donnell *et al.* (2011) cited evidence from a variety of measures of absolute velocity to propose a fast background model for theirs. Compilations of mean traveltime delays indicate that teleseismic *P* waves arrive early, not late beneath Ireland and the UK (Poupinet 1979; Poupinet *et al.* 2003; Amaru *et al.* 2008); global tomographic studies (Megnin & Romanowicz 2000; Montelli *et al.* 2006; Li *et al.* 2008) and regional surface-wave studies (Pilidou *et al.* 2004, 2005) all indicate that fast *P*- and *S*-wave velocity anomalies characterize the upper-mantle beneath the region. Although new constraints on seismic wave speed beneath the UK/Ireland may reveal genuinely slow velocity structure, the published literature on the region presently suggests otherwise. The proposed ∼200 °C thermal anomaly for the UK/Irish mantle would, in any case, plot towards the high end of the global temperature range of large igneous provinces and hotspots as determined from petrology (e.g. Rooney *et al.* 2012), which is somewhat unlikely given the paucity of recent volcanism and high heat flow in the region (e.g. Brock 1989).

3 ESTIMATING THE BACKGROUND MEAN

Some studies use constraints on absolute seismic wave speed structure, for example from surface-wave data, to help constrain their starting velocity model before tomographic inversion of relative arrival-times (e.g. Allen *et al.* 2002; Rawlinson & Fishwick 2011), but usually this information is not utilized and 'standard' Earth 1–D models are thus assumed instead. In these cases, in the absence of an over-determined inverse problem, and a data set of accurate error-free self-consistent absolute traveltimes, it is almost inconceivable that any tomographic model will successfully retrieve the true amplitudes of wave speed anomalies. However, global tomographic models (e.g. Megnin & Romanowicz 2000; Grand 2002; Ritsema *et al.* 2010) that use large data sets of absolute traveltimes and other closer measures of absolute velocity anomaly (e.g. surface-wave dispersion) can still be used to help place constraints on the background mean velocity structure of a region, before interpretation of a regional 'relative' tomographic image. Databases of mean traveltime anomalies recorded at long-running permanent seismograph networks can also be used to approximate the background velocity structure of a region (e.g. Poupinet 1979; Poupinet *et al.* 2003; Amaru *et al.* 2008).

Fig. 5 shows vertically averaged *S*-wave velocity anomalies in the depth range 0-410 km for permanent seismograph stations (including the GeoScope and GSN networks) presently operating around the world (Fig. 6). For permanent stations AAE and FURI in Ethiopia (Fig. 6), mean velocity anomalies are amongst the slowest on Earth (negative anomalies), emphasizing the differences in δV_S between the study of Bastow *et al.* (2008) and Ritsema *et al.* (2010), as discussed earlier. The converse is true for the Canadian studies of Sol *et al.* (2002) and Frederiksen *et al.* (2007): stations such as FRB and FFC on the Canadian shield (Fig. 6) are characterized by some of the largest amplitude fast wave speed anomalies on Earth.

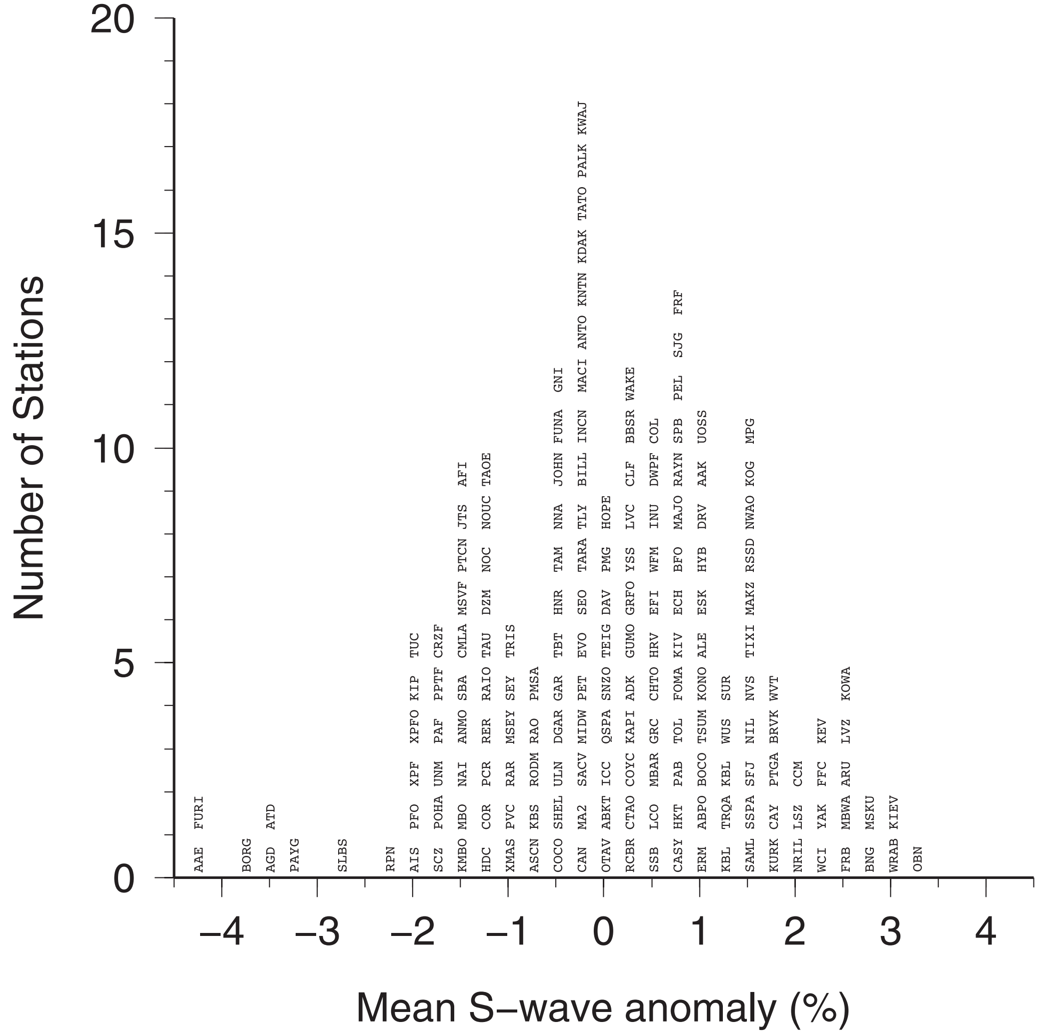

Figure 5. Panel (a) Histogram of mean shear wave velocity anomalies through the upper 410 km of the global tomographic model of Ritsema *et al.* (2010). Early arrivals, indicative of fast mantle seismic wave speeds are positive anomalies; late arrivals, indicative of slow mantle seismic wave speeds are negative anomalies. Stations OBN and AAE, shown in Fig. 6 are characterized by the fastest and slowest upper mantle wave speeds on Earth.

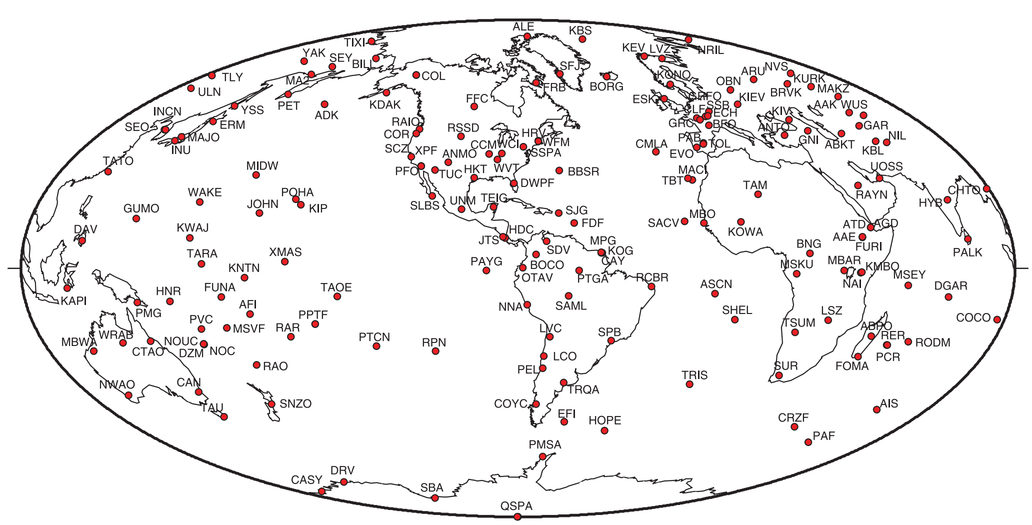

Figure 6. Locations of permanent seismograph stations for which mean upper-410 km *S*-wave velocity anomalies are presented in Fig. 5. Stations are part of permanent networks including Geoscope and GSN.

In the case of the aforementioned UK/Ireland studies, mean wave speed anomalies presented in Fig. 5, indicate fast velocity structure beneath permanent station ESK ($\delta V_S \approx 1$ per cent) in Scotland, which supports the conclusion of O'Donnell *et al.* (2011) that elevated temperatures and partial melt are not required to explain tomographic images there.

Global absolute velocity tomographic models, and traveltime catalogues, of course, provide only ball-park figures to help guide interpretation of the relative arrival-time images. Archean keels surrounded by slow asthenospheric mantle (e.g. Tanzania) are also genuinely fast wave speed anomalies (Ritsema *et al.* 1998) so the vertically averaged anomalies shown in Fig. 5 cannot always be used to benchmark precisely a regional 'relative' study. Future body-wave tomographic inversions in places like the UK/Ireland could usefully replace their 'global' starting model with one constrained *a priori* from absolute measures of velocity such as surface wave dispersion (e.g. Allen *et al.* 2002; Rawlinson & Fishwick 2011, for Iceland and Australia, respectively). On the other hand, studies of relative arrival-times alone remain valuable additions to the literature and should not be discouraged. Tomographers should, though, be abundantly clear what their low and high velocity anomalies mean in the context of the global average (see e.g. Schimmel *et al.* 2003; Bastow *et al.* 2005, 2008; O'Donnell *et al.* 2011). While the seismological community may be familiar with the difference between low and slow, and high and fast anomalies, the broader Earth Science community, who are often keen to interpret tomographic images for themselves, are almost certainly not.

4 CONCLUSIONS

Seismic tomographic studies that use relative, not absolute, arrival-time data to constrain seismic wave speeds yield models with a zero mean that corresponds to the average velocity structure of the region. There are very few places on Earth, however, where this zero velocity contour will coincide precisely with the $\delta V = 0$ per cent global average. Low wave speed anomalies should thus not necessarily be interpreted as 'slow', and high velocities should not necessarily be interpreted as 'fast' compared to the global mean. Brief consultation of absolute traveltime catalogues and global tomographic models can help constrain the elusive $\delta V = 0$ per cent contours in the relative arrival-time studies and thus aid interpretation of the results. Perhaps most importantly, such practice could help avoid confusion amongst the broader readership of the tomographic literature.

ACKNOWLEDGMENTS

I am grateful to advice from many people with whom I have discussed the problems with relative arrival-time tomography many times over the years, in particular J.P. O'Donnell, N. Rawlinson, D. Anderson, E. Daly, F. Darbyshire, J. Evans, G. Foulger and G. Houseman. Reviewers R. England and F. Tilmann, and editor G. Laski provided helpful comments that sharpened greatly the focus of the manuscript. IB is funded by the Leverhulme Trust.

REFERENCES

Aki, K., Christofferson, A. & Husebye, E.S., 1976. Three dimensional seismic structure of the lithosphere under Montana LASA, *Bull. seism. Soc. Am.,* **66,** 501–524.

Aki, K., Christofferson, A. & Husebye, E.S., 1977. Determination of the three-dimensional seismic structure of the lithosphere, *J. geophys. Res.,* **82,** 277–296.

Aki, K. & Richards, P.G., 1980. *Quantitative Seismology: Theory and Methods,* Vol. 2, Freeman Co., San Francisco, CA, 932pp.

Allen, R.M. *et al.*, 2002. Imaging the mantle beneath Iceland using integrated seismological techniques, *J. geophys. Res.,* **107,** 2325, doi:10.1029/2001JB000595.

Amaru, M.L., Spakman, W., Villasenor, A., Sandoval, S. & Kissling, E., 2008. A new absolute arrival time data set for Europe, *Geophys. J. Int.,* **173**(2), 465–472.

Anderson, D.L., 2011. Hawaii, boundary layers and ambient mantle—geophysical constraints, *J. Petrol.,* **52**(7–8), 1547–1577.

Arrowsmith, S.J., Kendall, J.-M., White, N. & VanDecar, J.C., 2005. Seismic imaging of a hot upwelling beneath the British Isles, *Geology,* **33**(5), 345–348.

Artemieva, I.M., Billien, M., Lévêque, J.J. & Mooney, W.D., 2004. Shear-wave velocity, seismic attenuation, and thermal structure of the continental upper mantle, *Geophys. J. Int.,* **157**(2), 607–628.

Bastow, I.D., Keir, D. & Daly, E., 2011. The Ethiopia Afar Geoscientific Lithospheric Experiment (EAGLE): Probing the transition from continental rifting to incipient seafloor spreading, *Geol. Soc. Am. Spec. Papers,* **478,** 51–76, doi:10.1130/2011.2478(04).

Bastow, I.D., Nyblade, A.A., Stuart, G.W., Rooney, T.O. & Benoit, M.H., 2008. Upper mantle seismic structure beneath the ethiopian hotspot: rifting at the edge of the African low velocity anomaly, *Geochem. Geophys. Geosyst*, **9**(12), Q122022, doi:10.1029/2008GC002107.

Bastow, I.D., Stuart, G.W., Kendall, J-M. & Ebinger, C.J., 2005. Upper-mantle seismic structure in a region of incipient continental breakup: northern Ethiopian rift, *Geophys. J. Int.,* **162,** 479–493.

Brock, A., 1989. Heat flow measurements in Ireland, *Tectonophysics,* **164**(2–4), 231–236.

Evans, J.R. & Achauer, U., 1993. Teleseismic tomography using the ACH method: theory and application to continental scale studies, in *Seismic Tomography: Theory and Practice,* eds. Iyer, H. & Hirahara, K., Chapman and Hall, New York.

Foulger, G.R., 2010. *Plates vs. Plumes: A Geological Controversy,* Wiley-Blackwell, Chichester, 364pp.

Frederiksen, A.W., Miong, S.W., Darbyshire, F.A., Eaton, D.W., Rondenay, S. & Sol, S., 2007. Lithospheric variations across the Superior Province, Ontario, Canada: evidence from tomography and shear wave splitting, *J. geophys. Res.,* **112**(B7), B07318, doi:10.1029/2006JB004861.

Goes, S., Govers, R. & Vacher, P., 2000. Shallow mantle temperatures under Europe from *P* and *S* wave tomography, *J. geophys. Res.,* **105**(B5), 11 153–11 169.

Grand, S.P., 2002. Mantle shear-wave tomography and the fate of subducted slabs, *Royal Soc. Lond. Phil. Trans. Ser. A,* **360,** 2475–2491.

Karato, S., 1993. Importance of anelasticity in the interpretation of seismic tomography, *Geophys. Res. Lett.,* **20**(15), 1623–1626.

Kennett, B. & Engdahl, E., 1991. Traveltimes from global earthquake location and phase identification, *Geophys. J. Int.,* **105**(2), 429–465.

Lévêque, J.J. & Masson, F., 1999. From ACH tomographic models to absolute velocity models, *Geophys. J. Int.,* **137**(3), 621–629.

Li, C., van der Hilst, R.D., Engdahl, R. & Burdick, S., 2008. A new global model for P wave speed variations in Earth's mantle, *Geochem. Geophys. Geosyst.,* **9**(5), Q05018, doi:10.1029/2007GC001806.

Megnin, C. & Romanowicz, B., 2000. The three-dimensional shear velocity structure of the mantle from the inversion of body, surface and higher-mode waveforms, *Geophys. J. Int.,* **143**(3), 709–728.

Montelli, R., Nolet, G., Dahlen, F.A. & Masters, G., 2006. A catalogue of deep mantle plumes: new results from finite-frequency tomography, *Geochem. Geophys. Geosyst.,* **7,** Q11007, doi:10.1029/2006GC001248.

Nakanishi, I. & Anderson, D.L., 1984. Aspherical heterogeneity of the mantle from phase velocities of mantle waves, *Nature,* **307**(5947), 117–121.

O'Donnell, J.P., Daly, E., Tiberi, C., Bastow, I.D., O'Reilly, B.M., Readman, P.W. & Hauser, F., 2011. Lithosphere–asthenosphere interaction beneath Ireland from joint inversion of teleseismic P-wave delay times and GRACE gravity, *Geophys. J. Int.,* **184,** 1379–1396.

Pilidou, S., Priestley, K., Debayle, E. & Gudmundsson, O., 2005. Rayleigh wave tomography in the North Atlantic: high resolution images of the Iceland, Azores and Eifel mantle plumes, *Lithos,* **79**(3–4), 453–474.

Pilidou, S., Priestley, K., Gudmundsson, O. & Debayle, E., 2004. Upper mantle S-wave speed heterogeneity and anisotropy beneath the North Atlantic from regional surface wave tomography: the Iceland and Azores plumes, *Geophys. J. Int.,* **159**(3), 1057–1076.

Poupinet, G., 1979. On the relation between P-wave travel time residuals and the age of the continental plates, *Earth planet. Sci. Lett.,* **43,** 149–161.

Poupinet, G., Arndt, N. & Vacher, P., 2003. Seismic tomography beneath stable regions and the origin and composition of the continental lithospheric mantle, *Earth planet. Sci. Lett.,* **212,** 89–101.

Priestley, K., McKenzie, D., Debayle, E. & Pilidou, S., 2008. The African upper mantle and its relationship to tectonics and surface geology, *Geophys. J. Int.,* **175**(3), 1108–1126.

Rawlinson, N. & Fishwick, S., 2011. Seismic structure of the southeast Australian lithosphere from surface and body wave tomography, *Tectonophysics*, in press, doi:10.1016/j.tecto.2011.11.016.

Rawlinson, N. & Kennett, B.L.N., 2008. Teleseismic tomography of the upper mantle beneath the southern lachlan orogen, Australia, *Phys. Earth planet. Inter.,* **167**(1–2), 84–97.

Ritsema, J., Deuss, A., Heijstvan, H.J. & Woodhouse, J.H., 2010. S40RTS: a degree-40 shear-velocity model for the mantle from new Rayleigh wave dispersion, teleseismic traveltime and normal-mode splitting function measurements, *Geophys. J. Int.,* **184,** 1223–1236, doi:10.1111/j.1365-246X.2010.04884.x.

Ritsema, J., Nyblade, A.A., Owens, T.J., Langston, C.A. & VanDecar, J.C., 1998. Upper mantle seismic velocity structure beneath Tanzania, East Africa: implications for the stability of cratonic lithosphere, *J. geophys. Res.,* **103**(B9), 21 201–21 213.

Ritzwoller, M.H., Shapiro, N.M., Barmin, M.P. & Levshin, A.L., 2002. Global surface wave diffraction tomography, *J. geophys. Res.,* **107**(B12), doi:10.1029/2002JB001777.

Romanowicz, B.A., 1979. Seismic structure of the upper mantle beneath the united states by three dimensional inversion of the body wave arrival times, *Geophys. J. R. astr. Soc.,* **57,** 479–506.

Rooney, T.O., Herzberg, C. & Bastow, I.D., 2012. Elevated mantle temperature beneath East Africa, *Geology,* **40,** 27–40.

Schimmel, M., Assumpção, M. & VanDecar, J.C., 2003. Seismic velocity anomalies beneath SE Brazil from P and S wave travel time inversions, *J. geophys. Res.,* **108**(B4), 2191, doi:10.1029/2001JB000187, 2003.

Sobolev, S.V., Zeyen, H., Stoll, G., Werling, F., Altherr, R. & Fuchs, K., 1996. Upper mantle temperatures from teleseismic tomography of French Massif Central including effects of composition, mineral reactions, anharmonicity and partial melt, *Earth planet. Sci. Lett.,* **139,** 147–163.

Sol, S., Thompson, C.J., Kendall, J.-M., White, D., VanDecar, J.C. & Asude, I., 2002. Seismic tomographic images of the cratonic upper mantle beneath the Western Superior Province of the Canadian Shield–a remnant Archaean slab, *Phys. Earth planet. Int.,* **134,** 53–69.

Takei, Y., 2002. Effect of pore geometry on $V_{\rm P}/V_{\rm S}$: From equilibrium geometry to crack, *J. geophys. Res.,* **107**(B2), doi:10.1029/2001JB000522.

Tanimoto, T. & Anderson, D.L., 1985. Lateral heterogeneity and azimuthal anisotropy of the upper mantle- Love and Rayleigh waves 100-250 sec, *J. geophys. Res.,* **90,** 1842–1858.

Tilmann, F.J., Benz, H.M., Priestley, K.F. & Okubo, P.G., 2001. P–wave velocity structure of the uppermost mantle beneath Hawaii from traveltime tomography, *Geophys. J. Int.,* **146,** 594–606.

van der Lee, S. & Fredericksen, A., 2005. Surface wave tomography applied to the North American upper mantle, in AGU Monograph "Seismic Earth: array Analysis of Broadband Seismograms", *J. geophys. Res.,* **157,** 67–80.

VanDecar, J.C., 1991. Upper-mantle structure of the Cascadia subduction zone from non-linear teleseismic travel time inversion, *PhD thesis*, University of Washington, Seattle, WA.

VanDecar, J.C. & Crosson, R.S., 1990. Determination of teleseismic relative phase arrival times using multi-channel cross–correlation and least squares, *Bull. seism. Soc. Am.,* **80**(1), 150–169.

VanDecar, J.C., James, D.E. & Assumpção, M., 1995. Seismic evidence for a fossil mantle plume beneath South America and implications for plate driving forces, *Nature,* **378,** 25–31.

Wawerzinek, B., Ritter, J.R.R., Jordan, M. & Landes, M., 2008. An upper-mantle upwelling underneath Ireland revealed from non-linear tomography, *Geophys. J. Int.,* **175**(1), 253–268.

Zhang, Y.S. & Lay, T., 1996. Global surface wave phase velocity variations, *J. geophys. Res.,* **101**(B4), 8415–8436.